URTeC: 3868150

Developing a High-Efficiency Method for Field-Scale Simulation of a Tight and Naturally Fractured Reservoir in the Williston Basin

Xincheng Wan*[1], Lu Jin[1], Todd Jiang[1], James A. Sorensen[1], Chenyu Wu[1], and Ahmed Merzoug[1], 1. Energy & Environmental Research Center, University of North Dakota

Abstract

Natural fractures are important for oil and gas production in tight reservoirs that are usually characterized by ultralow matrix porosity and permeability. Natural fractures can be characterized by core sample analysis, image logs, production data, and other data sets; however, some of these data may not always be available. Addressing the uncertainty of natural fractures in the modeling and simulation processes is challenging, especially for a field-scale simulation that requires intense computational efforts. The objective of this study was to develop a high-efficiency simulation workflow that quantifies drained reservoir volumes (DRVs) and reproduces the production and water injection history for a tight and naturally fractured reservoir in the Williston Basin.

The production history of all the wells and logging data were collected to characterize reservoir heterogeneity. Core samples from the target reservoir were tested to estimate petrophysical properties and identify natural fractures. The reservoir and fracture information was used to build a field-scale reservoir model. History matching was performed using a compositional reservoir simulator with the embedded discrete fracture modeling (EDFM) method. A fracture and DRV optimization (FDO) workflow was developed to improve history-matching results. The workflow enables dynamic updating of fracture and DRV parameters during history matching to reflect the change of key fracture properties in the production process.

Core sample analysis showed that the permeability of most samples ranged from 0.001 to 0.1 mD, with a few samples at a permeability higher than 1 mD. Cumulative oil production per well ranged from 17 to 200 thousand barrels (Mbbl). The results of permeability and cumulative oil production distribution indicated strong heterogeneity within the reservoir. Open fractures were detected from the tested core samples. Experimental and production data were integrated within the field-scale reservoir model. Assisted by the FDO workflow, the production and water injection histories for all 17 wells were successfully matched. The simulation results showed that water injection led to increasing water cut in two offset wells and restoration of reservoir pressure.

A novel FDO workflow was proposed in this study to better reproduce the production and water injection history of a tight reservoir with natural fractures in the Williston Basin. Compared to most of the published work in this area, the FDO workflow can significantly improve the simulation efficiency for field-scale

simulation models considering the presence of a complex natural fracture network. The workflow can be further applied to reservoir fracture network characterization and history matching of other unconventional reservoirs with complex natural fracture systems.

Introduction

Naturally fractured reservoirs, particularly with tight matrices, are becoming an important source of oil and gas production. These reservoirs are often characterized by low to ultralow matrix porosity and permeability, making it challenging to produce oil and gas from the matrices directly. The presence of natural fractures plays an essential role in enhancing reservoir permeability and facilitating oil and gas flow toward wellbores (Narr et al., 2006). Therefore, it is crucial to understand the presence and characteristics of natural fractures.

A variety of data, including core, image log, seismic, and well-testing interpretations, can be utilized to better understand natural fractures. Core sample analysis is a direct method to determine the origin, presence, geometry, and mineralization of natural fractures (Gale et al., 2019). Image logs can be used to visualize fracture orientation, frequency, and continuity (Fernández-Ibáñez et al., 2018). The combination of core sample analysis and image log provides precise and detailed data on fracture geometry and occurrence (Narr et al., 2006; Ibrayev et al., 2016). However, they cannot determine whether the well-scale natural fractures are connected to a field-scale natural fracture system to allow gas and fluids to flow into wellbores. Seismic data can provide structure, geometry, and geomechanical properties of large natural fractures on the field scale, but they cannot detect small natural fractures (Lynn et al., 1995; Ibrayev et al., 2016). In addition, fracture connectivity or conductivity cannot be determined by seismic data. In contrast, well-testing data can characterize the flow capacity of natural fractures and evaluate heterogeneity in naturally fractured reservoirs (Cinco-Ley, 1996) but cannot determine the occurrence or geometry of natural fractures. Although a better characterization of natural fractures can be obtained by utilizing all types of data, these data sets are usually not available for most fields because of the high cost of acquiring the data in actual fields (Narr et al., 2006; Ray et al., 2012). Therefore, developing a high-efficiency method to mimic the flow behavior in naturally fractured reservoirs becomes meaningful and can assist operators to improve oil and gas production and maximize economic benefits when developing these reservoirs.

Reservoir simulation is the key to characterizing the fluid flow behavior of tight naturally fractured reservoirs; however, the modeling and simulation process can be challenging (Oliver and Chen, 2011). One of the main challenges is how to simulate fractures efficiently. The conventional dual-porosity dual-permeability (DP/DK) method can simulate reservoirs with uniformly distributed natural fractures on a small scale; however, this method can provide inaccurate solutions when the simulated reservoir is highly heterogeneous with a complex natural fracture system (Warren and Root, 1963; Choi et al., 1997; Nie et al., 2012; Yu et al., 2014). The local grid refinement (LGR) and unstructured grid (UG) methods are also used to simulate fractured reservoirs, but these methods usually require long computational time, especially when there are multiple wells involved in the model (Conlin et al., 1990; Mirzaei and Cipolla, 2012; Sun et al., 2016; Jin et al., 2019). The embedded discrete fracture model (EDFM) method takes advantage of DP/DK, LGR, and UG methods to ensure that the simulation of a tight naturally fractured reservoir is accurate and efficient (Xu et al., 2017; Wan, 2020; Wan et al., 2020; Jin et al., 2022a, b). More recently, a machine learning-assisted automatic history-matching (AHM) algorithm was proposed to further enhance the EDFM method. The algorithm can generate an ensemble of solutions to address uncertainties of natural fracture properties in the history-matching process (Tripoppoom et al., 2019; Liu, 2020; Liu et al., 2022; Wan et al., 2022). However, this approach has two limitations: 1) a longer simulation time is required for uncertainty analysis and 2) the performance of AHM strongly depends on the quality of the baseline model; poor or no solution can be achieved when a reasonable baseline model is not available.

Simulation practices showed that the EDFM method is efficient in matching early-stage production data; however, matching efficiency reduces with time because of the depletion of the reservoir. Studies showed

that the properties of natural fractures and their neighboring matrices change with reservoir pressure in the production process (Tao et al., 2011; Cho et al., 2013; Zhao et al., 2017; Jia et al., 2020, 2021). These observations indicated an alternative method is needed to improve history-matching efficiency when the reservoir depletes. Therefore, this study aimed to develop a high-efficiency method for field-scale reservoir simulation of a tight and naturally fractured reservoir in the Williston Basin. The method can be further extended to other unconventional reservoirs with complex natural fractures if it can be successfully applied to the target reservoir.

Reservoir Overview

The studied Field A is a tight oil reservoir located in the North Dakota portion of the Williston Basin. The Ratcliffe interval of the Charles Formation is the main pay zone of the reservoir and one of the primary hydrocarbon-producing intervals within the Madison Group in North Dakota, along with the Lodgepole Formation and the Frobisher–Alida interval of the Mission Canyon Formation (Hendricks, 1988; Jarvie et al., 2016). The reservoir contains primarily low-porosity, low-permeability, fractured marine limestones and dolomites occurring at depths of approximately 8800–10,000 ft. Figure 1 shows different well logs collected from a well completed in the pay zone. Figure 2 provides porosity and permeability from core sample measurement for the corresponding well. Generally, the porosity of the pay zone is lower than 10%, with only a few thin layers exhibiting porosity greater than 10%. The permeability is in the range of 0.001–20 mD, with most of the pay zone showing a permeability of less than 0.1 mD. These figures indicate that this deep reservoir is not only tight but also strongly heterogeneous.

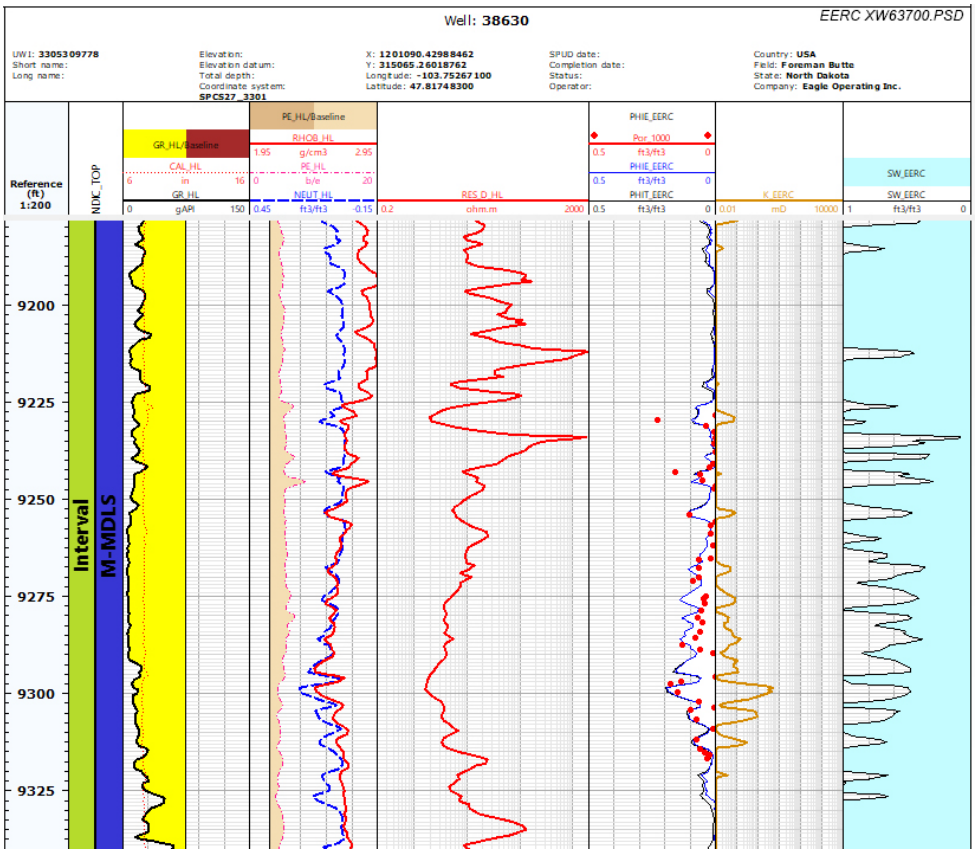

Figure 1. Well logs collected from one of the wells in Field A, with porosity log-matched by core data.

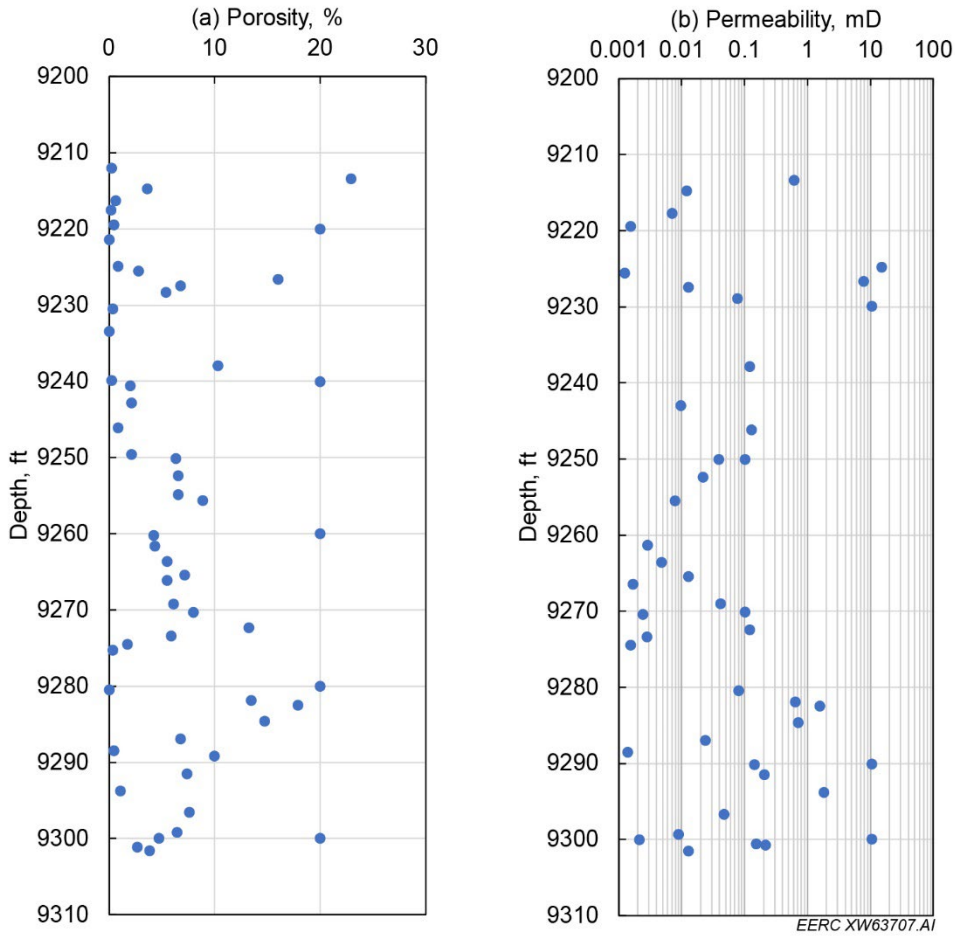

Figure 2. Distribution of porosity (a) and permeability (b), with depth based on core measurements.

Natural fractures were observed on the core samples obtained from the reservoir, as illustrated in Figure 3. The left three core samples show that the natural fractures are randomly distributed in different geometries and orientations – both vertical and horizontal fractures with different lengths appear on these samples. For comparison, the fourth core sample on the right-hand side shows an intact rock without the presence of natural fractures. Drilling and production activities showed that natural fractures are distributed across the reservoir in the Ratcliffe interval (Hirsch et al., 1981; Woo and Cramer, 1984; Begnaud and Claiborne, 1985).

Shell recovered over 1500 feet of core samples from three wells at the Mondak Field to analyze the natural open fractures in the interval (Hirsch et al., 1981). To delineate these fractures using wireline logs, the company ran the commercially available logging tools as well as the prototype devices designed to respond to open fractures. The results showed that most of the open natural fractures observed on the core samples are vertical, with a length ranging from several inches to several feet and a width typically less than a fraction of a millimeter. Begnaud and Claiborne (1983) observed that natural fractures played varying roles in oil production from reservoirs in the Mission Canyon and Ratcliffe units and that fracture properties might change with time as production went on. They reviewed the completions and production data of the wells in these geologic units and found that different methods were required to analyze the fractures depending on the rock properties and production history. They utilized seven field techniques, including zone testing, downhole pressure measurements, residual gel analysis, pump-in and swab tests, postfrac temperature logs, postfrac gamma ray logs, and drillstem test, and four stress measurements, including

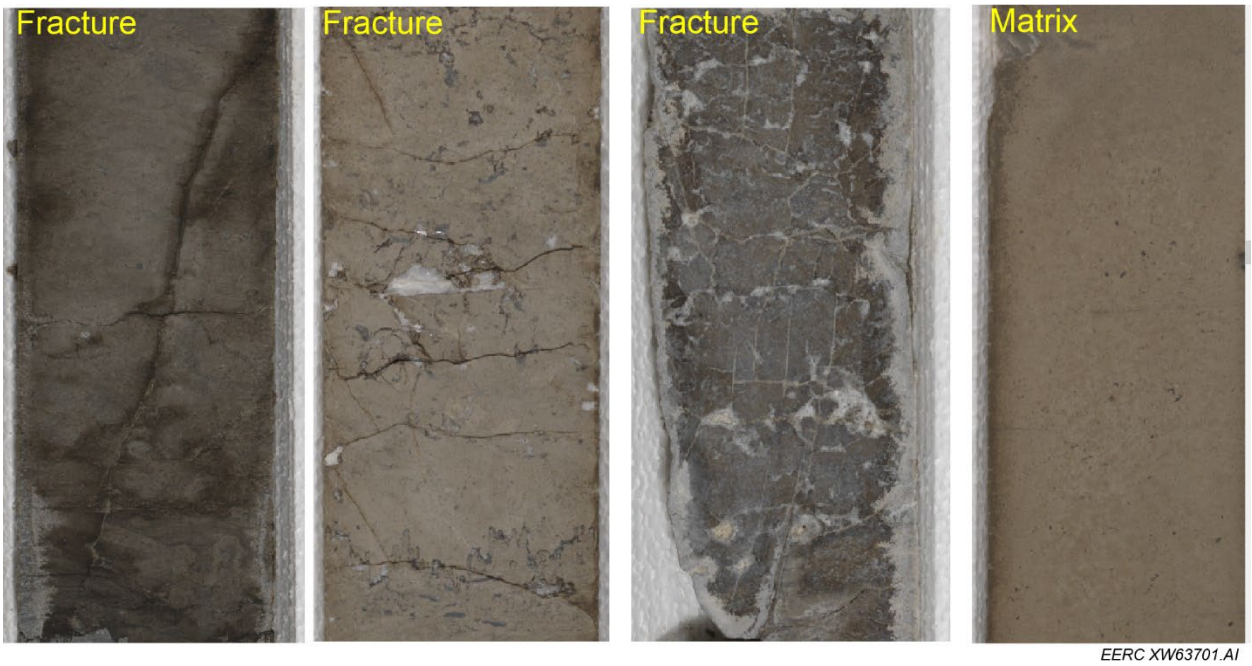

Figure 3. Illustration of natural fractures observed on the core samples collected from the reservoir.

horizontal stress, vertical stress, in situ closure stress, and long-spaced sonic log stress, to analyze vertical fracture growth in the studied reservoirs. Based on the analysis of the data collected from the reservoirs, they proposed the following correlation to predict the fracture height during the production process:

$$P - P_o = \frac{K_{ic}}{\sqrt{\pi L}} \frac{1}{\sqrt{1+\varepsilon}} - 1 + \frac{2(\sigma_b - \sigma_a)}{\pi} cos^{-1}\left(\frac{1}{1+\varepsilon}\right) \quad \text{[Eq. 1]}$$

Where P_o is the pressure as a fracture initially reaches the boundary, *psi*; P is the pressure above P_o, *psi*; L is half of the pay zone thickness, *ft*; ε is calculated as *(fracture half height/L-1)*, *ft*; K_{ic} is the critical stress intensity factor of the bounding layer; σ_b is the minimum horizontal stress in the pay zone, *psi*; and σ_a is the minimum horizontal stress in the boundary, *psi*.

Since the stresses changed with pore pressure (or reservoir pressure) in the production and injection process, the fracture height was not constant throughout the life cycle of a field. The production and injection history should be considered when estimating the fracture properties. Begnaud and Claiborne (1983) estimated that the natural fracture height could vary between 0 and 100 ft in the studied reservoirs depending on the pressure conditions. Therefore, this factor needs to be considered in the fracture simulation process when studying reservoirs in the Ratcliffe interval.

Analysis of Production and Injection Data

Seventeen horizontal wells from Field A were selected to develop an effective simulation workflow for a naturally fractured reservoir in the Ratcliffe interval, as shown in Figure 4. The wells were drilled from 2004 to 2006 and then started oil production with openhole completions. The horizontal laterals were completed at an average depth of 9500 ft and an average length of 5300 ft. A large variation in initial oil production rate and cumulative oil production was observed in these wells: initial oil production rates ranged 52 to 515 bpd and cumulative oil production ranged 17 to 200 Mbbl, as shown in Figure 5. All of the wells had high initial water cuts ranging from 25% to 85%, as shown in Figure 6. A clear correlation could be observed between the initial water cut and cumulative oil production for these wells, as demonstrated in Figure 7. These observations indicated that the oil saturation distribution in the reservoir is highly uneven and the main pay zone might be in a transition zone with high water saturation.

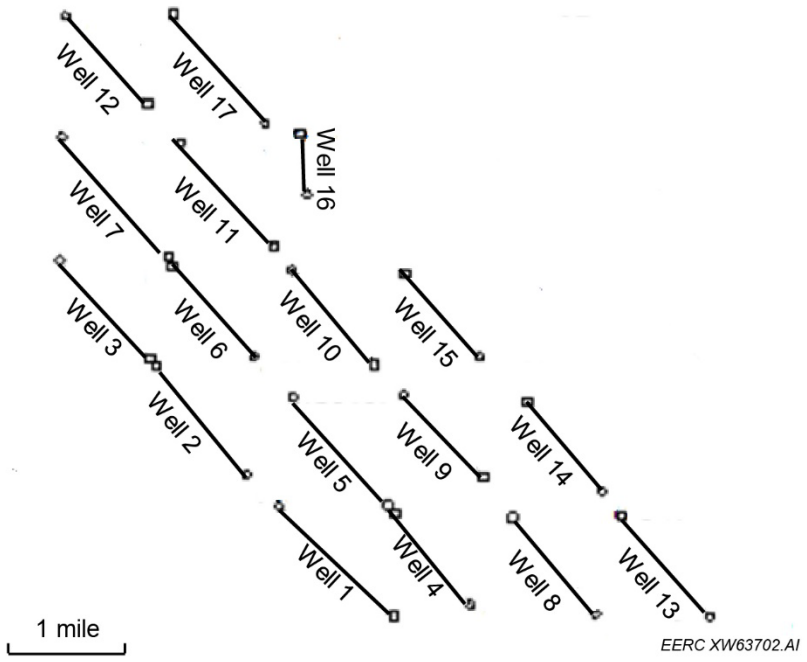

Figure 4. The 17 horizontal wells selected from Field A where the main pay zone is in the Ratcliffe interval.

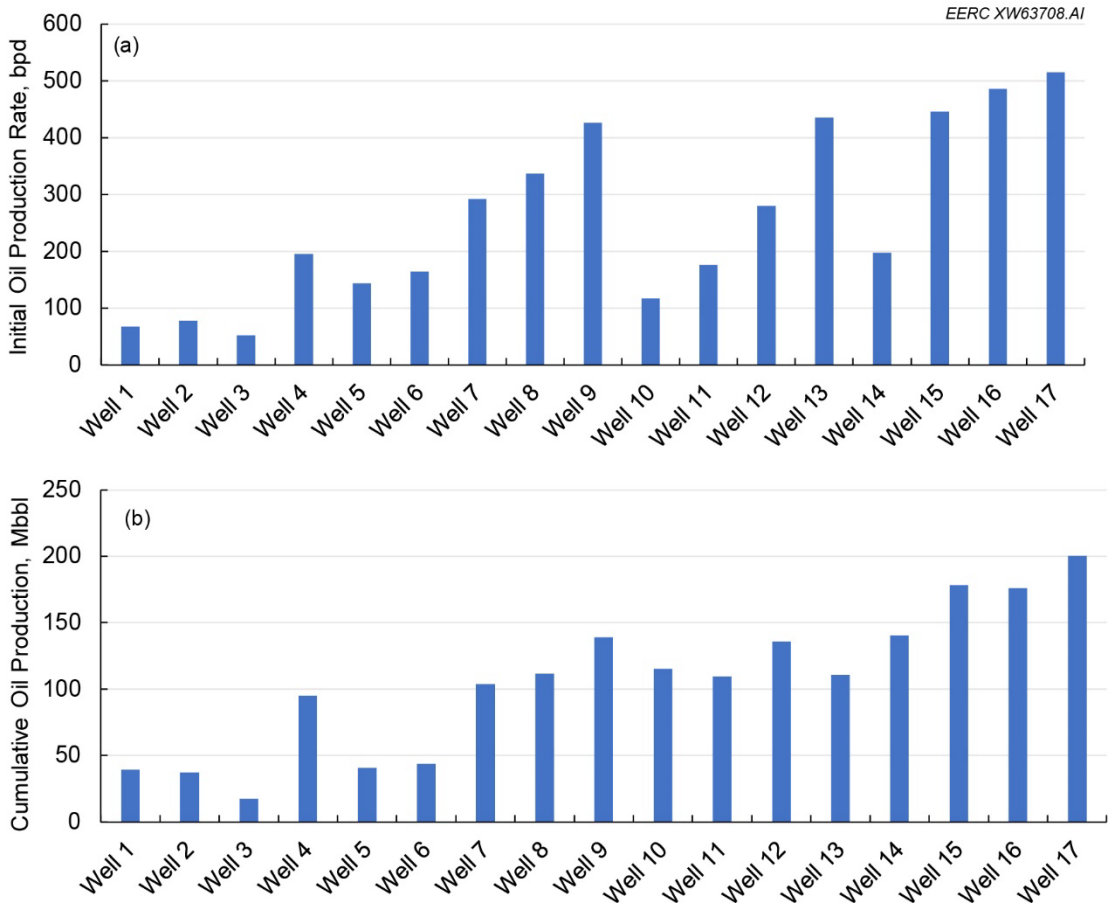

Figure 5. Oil production performance of the selected wells in Field A: (a) initial oil production rate and (b) cumulative oil production.

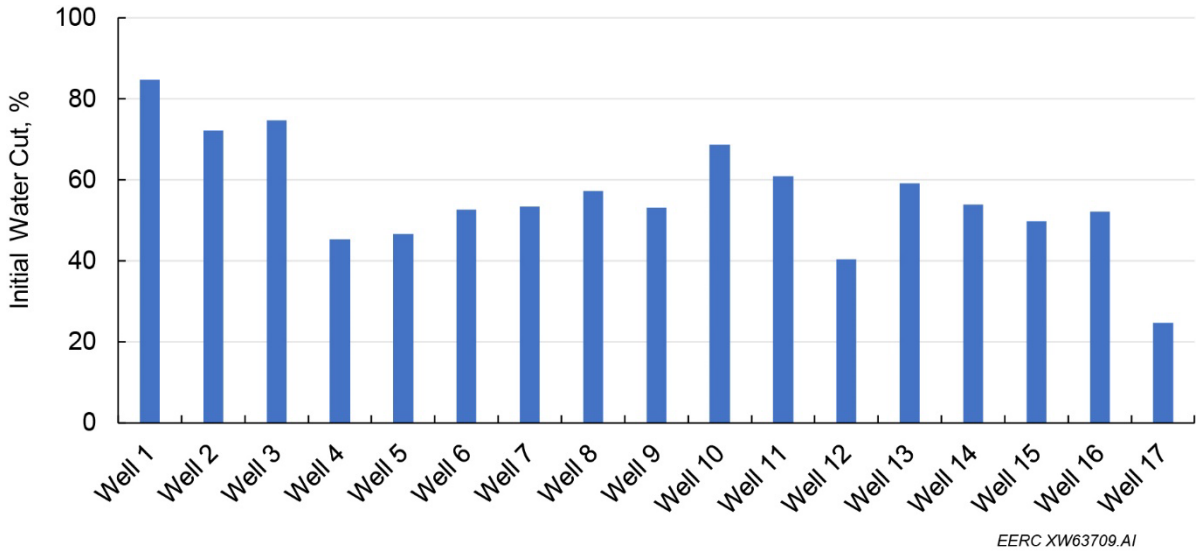

Figure 6. Initial water cut of the 17 wells in Field A.

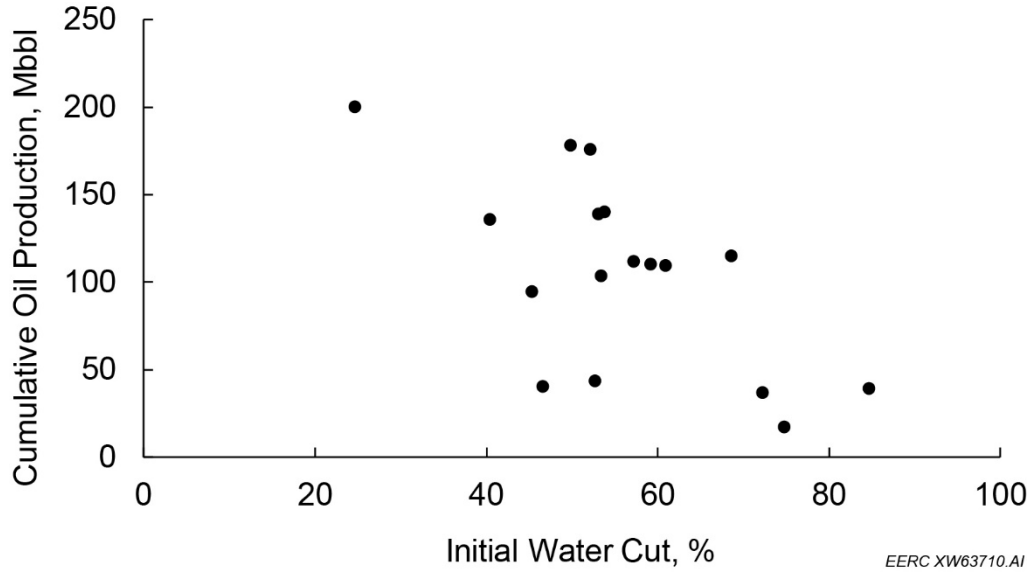

Figure 7. Correlation between initial water cut and cumulative oil production for the 17 wells in Field A.

A transition zone is a region where oil and water are intermixed and the water saturation changes gradually from 100% to connate saturation as the oil saturation increases. Capillary pressure is defined as the difference in fluid pressure across an interface between two fluids in a confined volume. In an oil reservoir, it is the pressure difference across the oil–water interface, which is a function of the fluid and rock properties. Capillary pressure plays a crucial role in determining the thickness of a transition zone. Studies showed that the thickness of a transition zone may vary from a few feet in high-permeability reservoirs to more than 300 feet in low-permeability reservoirs such as carbonate reservoirs because of extreme heterogeneity (Masalmeh et al., 2007; Bera and Belhaj, 2016; Shi et al., 2018; Dakhelpour-Ghoveifel et al., 2019).

The transition zone may hold a substantial portion of oil reserves in a reservoir, where the oil production performance and recovery depend heavily on several geological and petrophysical properties based on special core analysis (SCAL) such as pore size distribution, capillary pressure, and relative permeability (Spearing et al., 2014; Mohamed et al. 2017; Shi et al., 2018). Capillary pressure is one of the most important factors to understand the fluid flow behavior in a transition zone. Capillary pressure data can

provide valuable information on the size and sorting of pore throats and the pressure difference required to move fluids through the pores (Jin and Wojtanowicz, 2014; Bera and Belhaj, 2016; Zhang et al., 2019, 2020). Therefore, high-pressure mercury injection (MICP [mercury injection capillary pressure]) tests were performed to measure the capillary pressure in this reservoir. Figure 8 illustrates a capillary pressure curve that was measured by MICP using a representative core sample from the reservoir with a porosity of 0.11 and a permeability of 0.45 mD. The curve indicates that a high pressure differential is required to displace oil through a large portion of pore throats in this reservoir. The steep change of the slope implies that oil is difficult to produce in the deeper transition zone since an extremely high pressure differential is required to overcome the capillary force between oil and water in the pore throats.

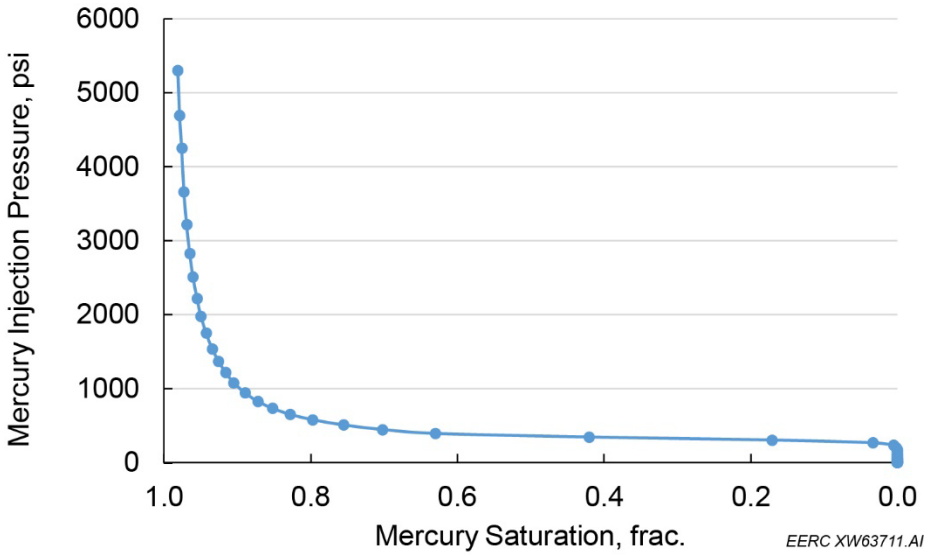

Figure 8. Capillary pressure curve measured by MICP using a core sample with a porosity of 0.11 and a permeability of 0.45 mD.

Water injection has been performed in Well 5 since October 2017, as shown in Figure 9. Data indicated that the maximum injection rate was limited to around 1650 bpd because of the low-permeability rock matrix surrounding the well. Wells 1, 2, and 6 have been shut in since 2013 because of their low oil production rates. Oil and water production responses have been monitored in offset Wells 4, 8, 9, and 10. Little change in water cut was observed in Wells 4 and 8, indicating that the communication between the injection well and these two production wells was weak. Conversely, increasing water cut was observed in Wells 9 and 10 after water injection started, as shown in Figure 10, implying that high-conductivity channels probably existed between Well 5 and Wells 9 and 10. The production and injection data further confirmed that the reservoir is highly heterogeneous. Accurately predicting the behavior of fluid flow in the reservoir was challenging because of the uncertainties in the distribution of permeability, porosity, initial oil saturation, and natural fractures across the reservoir. To address this challenge, a simulation workflow was developed to tune the matrix and fracture properties through detailed history matching.

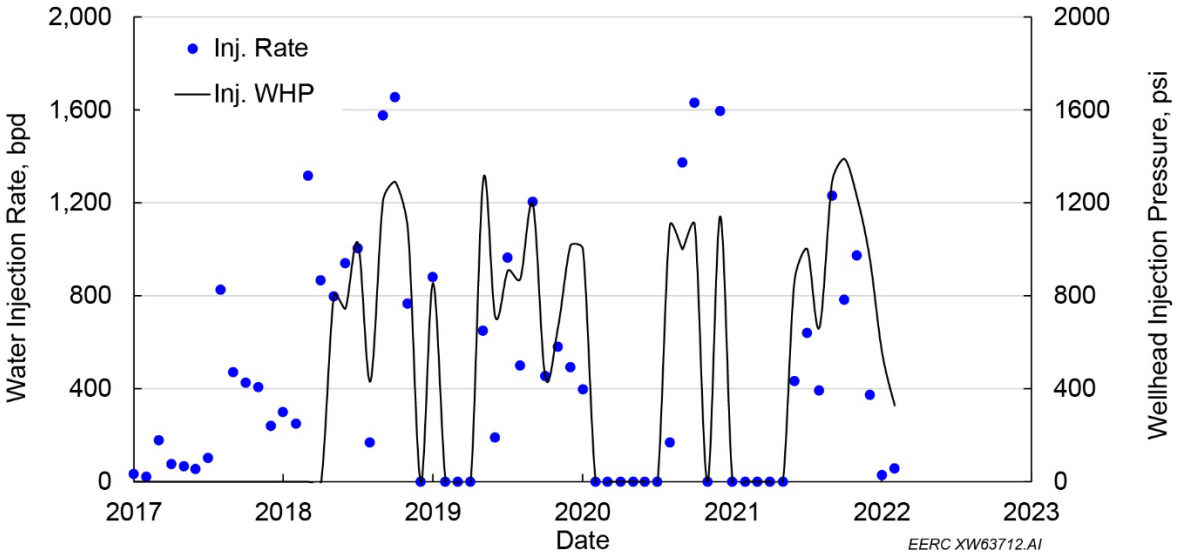

Figure 9. Water injection performance in Well 5.

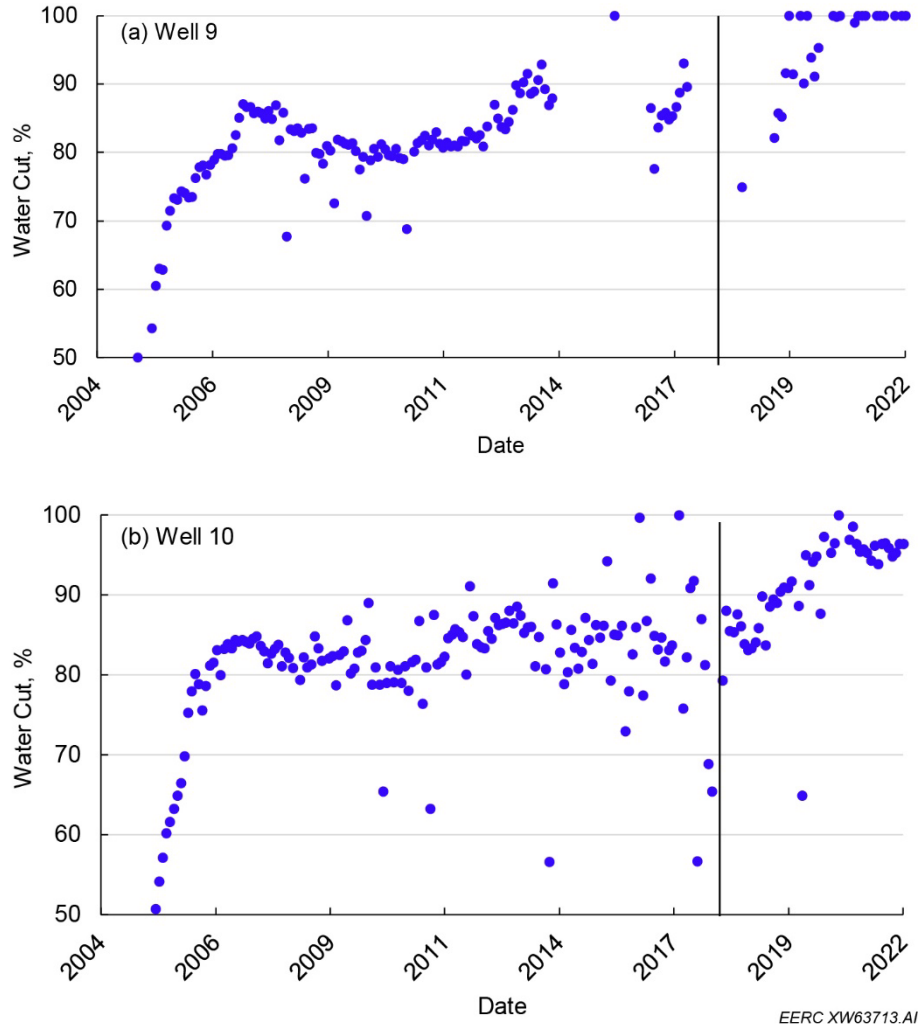

Figure 10. Change of water cut in offset wells after water injection started: (a) Well 9; (b) Well 10. The black line indicates water injection started in Well 5.

Baseline Model Description

To mimic the fluid flow behavior in the reservoir, a compositional reservoir simulation model was built using Computer Modelling Group Ltd.'s (CMG's) GEM®. All 17 wells shown in Figure 4 were included in the model. The length, width, and height of the original reservoir model (natural fractures) were approximately 40,350, 16,350, and 100 ft, with 135, 55, and 45 grids in the X, Y, and Z directions, respectively. The total bulk volume of the reservoir model is 7.29×10^7 ft^3. The geologic model was constructed using corner grids in Petrel® based on available well log and core data to assign initial values for porosity, permeability, and oil saturation, as shown in Figure 11. The distribution of porosity and permeability depicts the tight and heterogeneous features of the reservoir, as illustrated in Figure 11(a) and (b). Most of the reservoir matrix exhibited low porosity (less than 10%) and permeability (less than 0.1 mD), with a few thin layers showing higher porosity (≥10%) and permeability (≥0.1 mD). The oil saturation distribution confirmed that the reservoir was in a transition zone with high water saturation; Figure 11(c) shows that most of the reservoir had an initial oil saturation lower than 0.5. Additionally, the figure depicts a decreasing trend in oil saturation with increasing depth, where the effect of gravity on oil migration is clear. The distribution of reservoir properties correlated well with the oil production and water cut behaviors shown in Figure 5 through Figure 7.

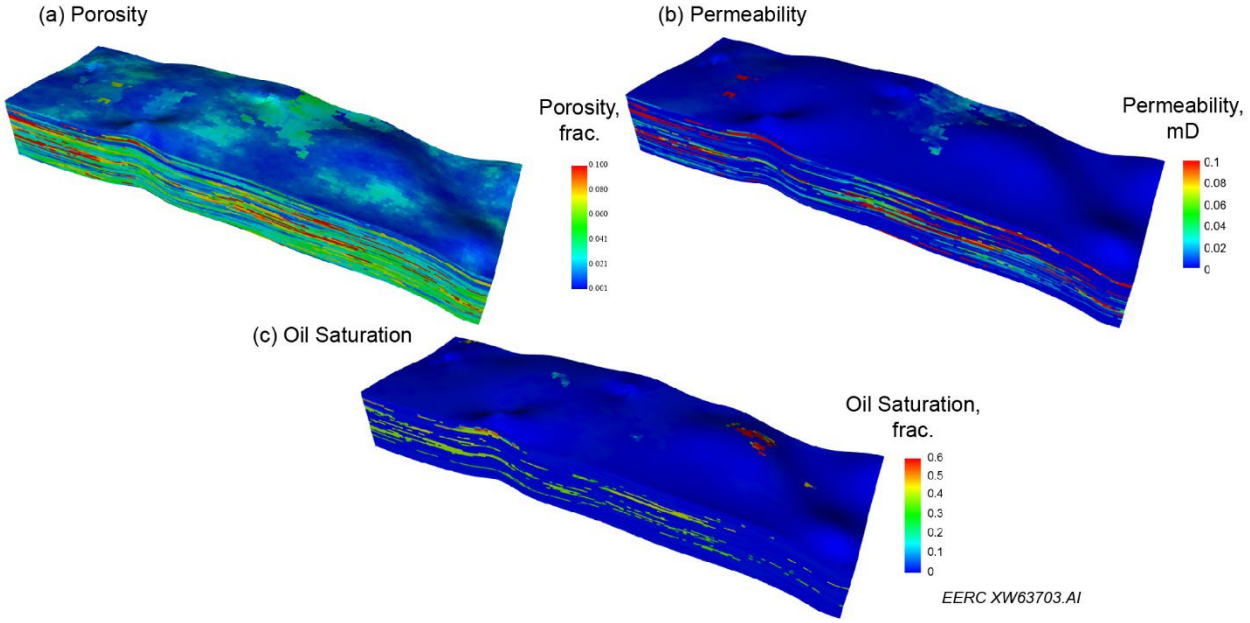

Figure 11. Distribution of different reservoir properties in the simulation model: (a) porosity, (b) permeability, and (c) water saturation. The height of the reservoir model was amplified 50 times to better display the vertical distribution of the reservoir properties.

Since many wells and natural fractures were involved in the model, selecting a high-efficiency fracture simulation method became a precondition for history matching. The EDFM approach was effective to integrate natural fractures into a reservoir simulation model. Different from most fracture simulation methods, EDFM constructed all fractures explicitly by separating the fracture matrix grids independently. The fractures were divided into segments and then connected using non-neighboring connections (NNCs) to make sure the fluid can flow through the fractures. This treatment greatly improved flow calculation efficiency in the simulation process (Xu, 2015; Lie and Møyner, 2021; Zhao et al., 2022). Fracture and matrix grids were then coupled to each other via source–sink relations when the simulation model was finalized. EDFM homogenized small natural fractures by adjusting the length, width, porosity, permeability, and transmissibility when tuning the model to make the simulation model run smoothly (Ma et al., 2022). This hierarchical modeling approach made EDFM versatile and convenient to handle complex fracture networks. Employing the EDGS® Suite, Figure 12 shows the simulation model of the studied reservoir with wells and natural fractures integrated.

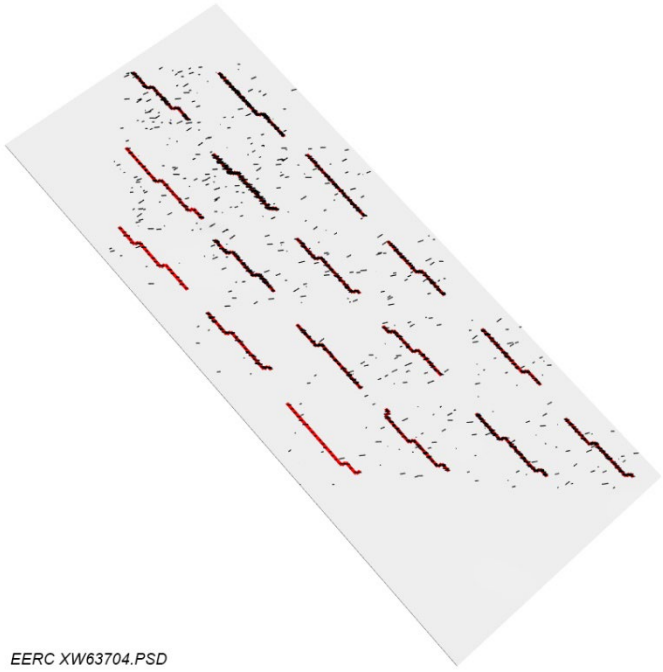

Figure 12. Distribution of wells and natural fractures in the simulation model.

Workflow Development

Because of the uncertainties in rock and natural fracture properties, initial simulation results deviated from historical data. Only adjusting the matrix properties could not make the model match the historical data satisfactorily; however, the initial simulation runs showed that the results were sensitive to the grids in the near-wellbore region. Tuning the natural fracture properties showed that simulation results were close to historical data, especially in the early stage of production. Later on, the matrix properties within the drained reservoir volume (DRV) became more influential on fluid flow behavior. These observations indicated that 1) the properties of natural fractures should be mainly adjusted for early-stage history matching, 2) the main DRV of each well might surround the wellbore because of the tightness of the rock matrix in the reservoir, and 3) the rock matrix properties in the DRV were mainly responsible for late-stage history matching. Therefore, a fracture and DRV optimization (FDO) workflow (Figure 13) was proposed to optimize the history-matching quality for this tight and naturally fractured reservoir.

The workflow began with an initialization of the simulation model to make sure the model could run through the available production history in a reasonable time. The essential matrix and fracture parameters such as porosity, permeability, and fluid saturations were tuned based on available well logs, core measurements, etc. When the model was able to run through smoothly, the results were compared with historical data and the model was kept as a baseline model. If the results were satisfied, i.e., met accuracy requirements, history matching was completed. If the simulation results deviated from historical data, then the properties of the near-wellbore grids mainly focused on natural fractures were tuned to match the production data for the early production period.

When the data of the early production period were matched, the properties of grids beyond the near-wellbore region were tuned to match the remaining historical data. The impact of matrix properties became more important for late-stage production. Figure 14 illustrates a DRV near a natural fracture. Based on the fracture grids that were generated in EDFM, all matrix cells that are connected to the fractures were

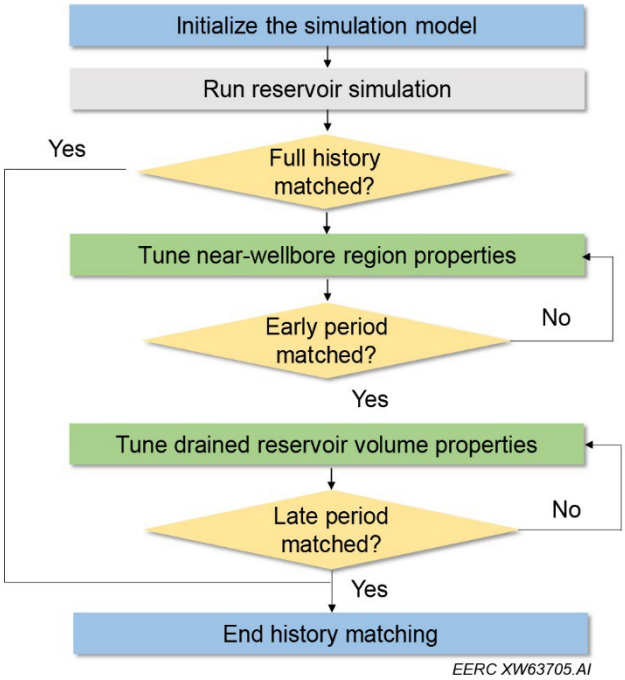

Figure 13. Simulation workflow for tight and naturally fractured reservoir history matching.

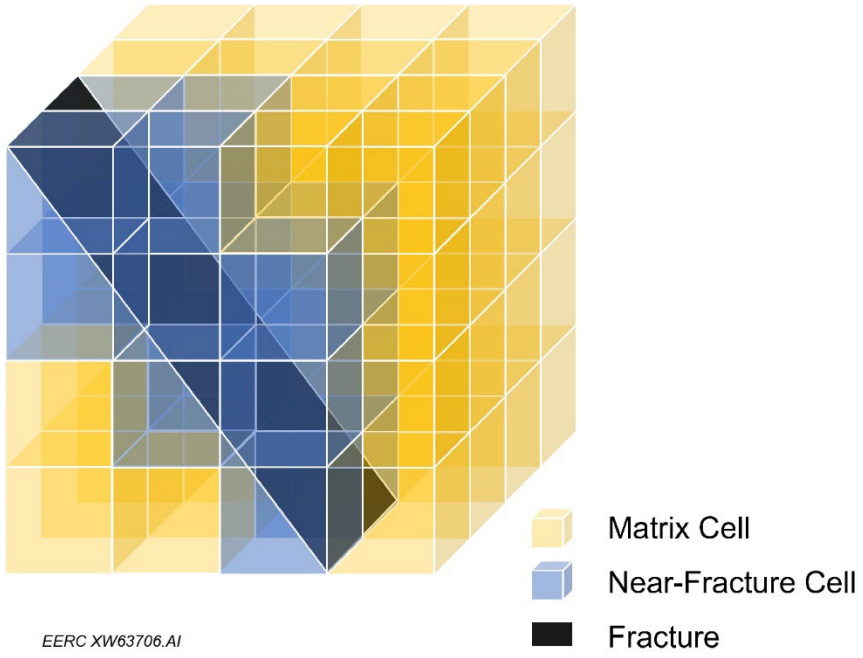

Figure 14. Illustration of a DRV near a natural fracture: the black piece represents a natural fracture embedded in the reservoir matrix, the blue blocks represent the cells that are directly connected to the fracture, and the yellow blocks represent the matrix cells that are not directly connected to the fracture.

identified and grouped based on their connected fractures. Properties such as permeability, relative permeability curves, and transmissibility were tuned in these cells to match historical data. Some natural fracture properties such as length, width, and permeability might also be tuned in this stage. The matrix cells were also updated when the length or width of their connected fracture was tuned; as a result, the DRV was updated. The updated reservoir model was then rerun and compared to historical data until a satisfactory history match was achieved.

History-Matching Results

Detailed history matching was performed for the 17 wells based on the workflow proposed in this study. Reasonable production history-matching results, including liquid rate, oil rate, and water rate, were achieved for both field and individual wells, as shown in Figure 15 through Figure 18. Because of a lack of gas compositional data, the gas production rate was not set as an objective for history matching. However, this did not impact the verification of the proposed method in this study. The liquid production rate was set as the primary production constraint. Therefore, the liquid rate was almost perfectly matched for all the wells, as demonstrated in Figure 15(a), Figure 16(a), and Figure 17(a). This indicated that the grids in the model had adequate conductivity to deliver the fluid volume. The plots on oil and water production rates showed slight but acceptable variations between the simulation results and production history. The matching results indicated that the simulation model could effectively mimic the fluid flow in this reservoir. The variations between the simulation and production also implied there were still uncertainties in the fracture and matrix properties and the simulation results could be further improved when more data are available to reduce the uncertainties.

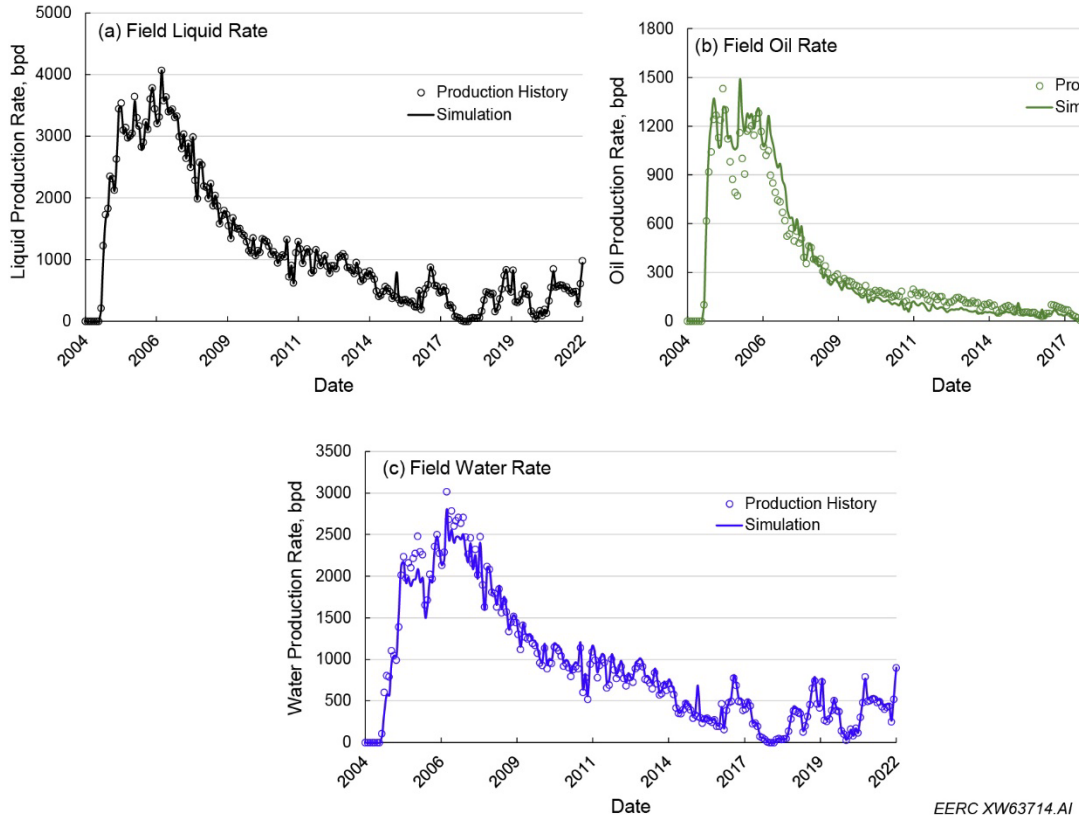

Figure 15. History-matching results for production rates in Field A: (a) liquid rate, (b) oil rate, and (c) water rate.

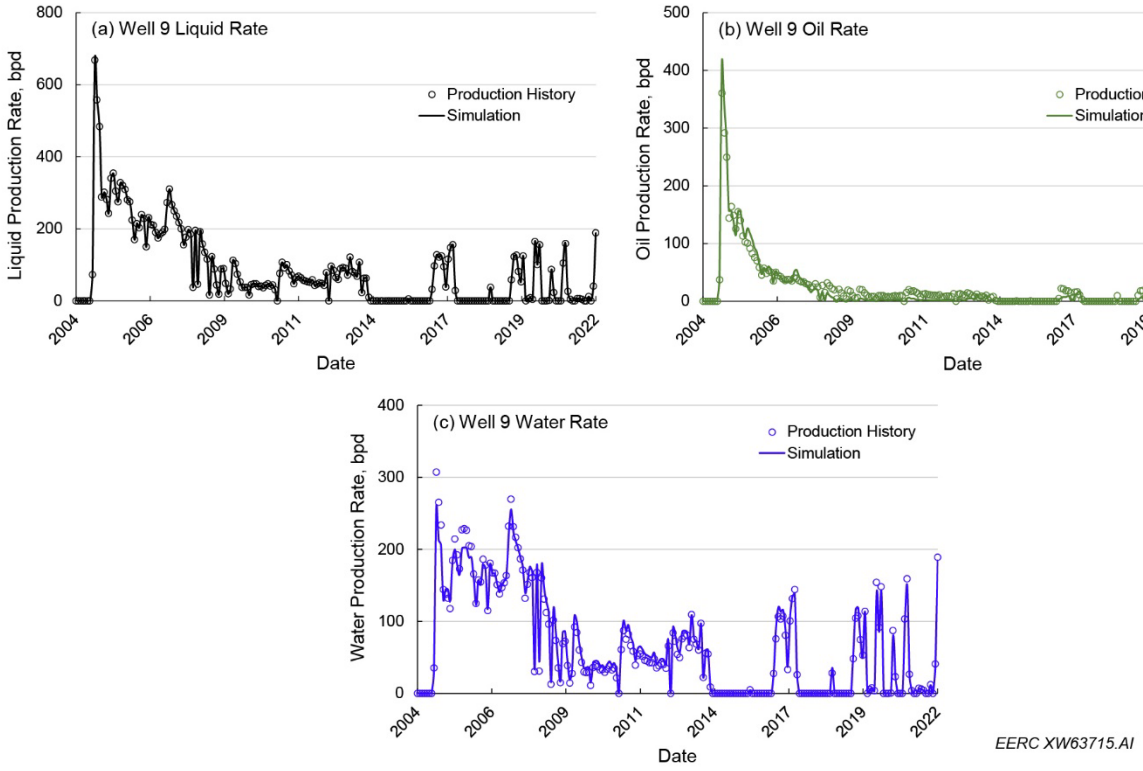

Figure 16. History-matching results for production rates in Well 9: (a) liquid rate, (b) oil rate, and (c) water rate.

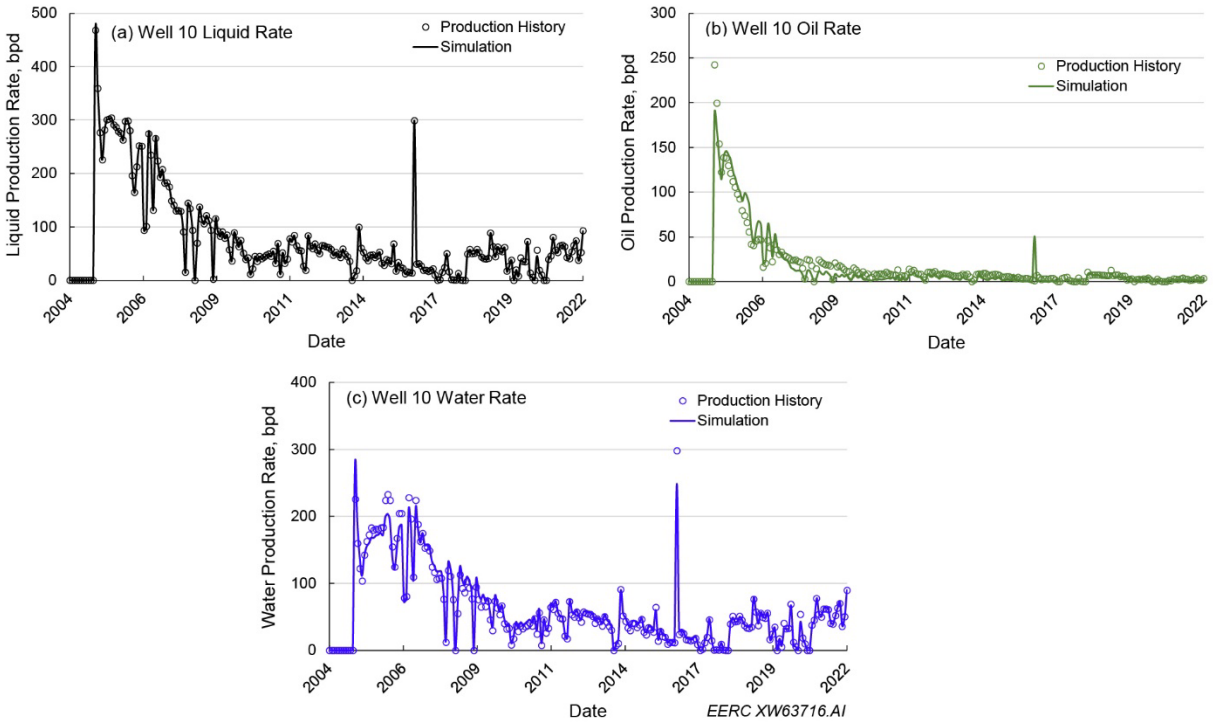

Figure 17. History-matching results for production rates in Well 10: (a) liquid rate, (b) oil rate, and (c) water rate.

Well 5 was the only water injection well in this field. Figure 18 shows that the simulation model could also match the water injection rate satisfactorily. Although the water injection caused an increasing water cut in offset Wells 9 and 10, as shown in Figure 10, it could potentially restore reservoir pressure, as indicated in

Figure 19. Average reservoir pressure decreased from 4400 to 2000 psi after 13 years of production. Water injection changed the declining trend, and there was a slight increase in reservoir pressure from 2019. However, the pressure increase was not significant since the water injection rate was limited because of the tightness of the reservoir and liquid production continued in other wells.

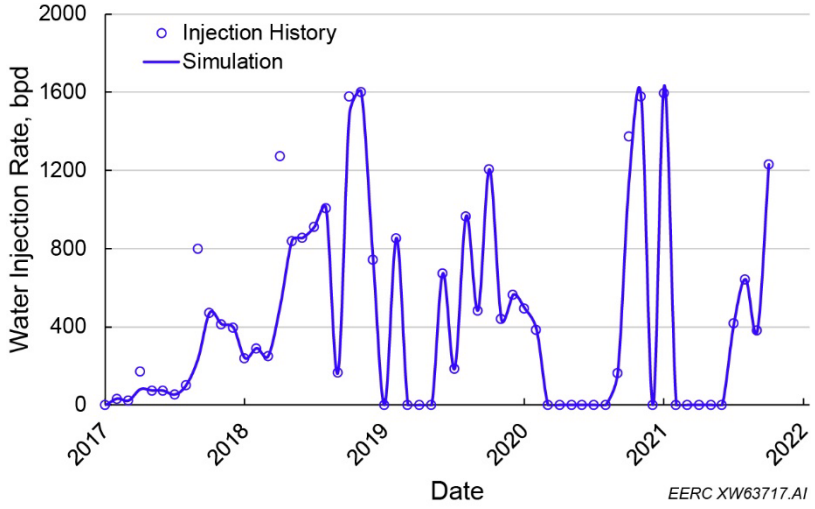

Figure 18. History-matching results for water injection rate in Well 5.

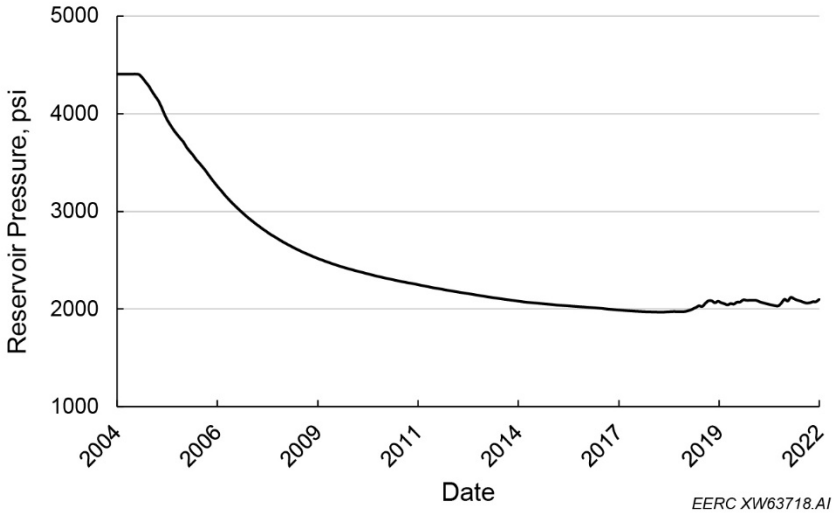

Figure 19. Simulation results of reservoir pressure decline in Field A.

Conclusions

This study applied multiple approaches to characterize fluid flow behavior in a tight and naturally fractured reservoir in the Williston Basin. Core samples, well logs, and production data were collected to analyze the porosity, permeability, natural fractures, and heterogeneity of the reservoir. A simulation model with complex natural fractures and 17 horizontal wells was built to reproduce production history. To better address the uncertainty of near-fracture matrix properties and achieve history matching more efficiently, a novel fracture and drained volume simulation workflow was proposed based on the EDFM method. The main findings of this study are summarized as follows:

1. With the assistance of the proposed simulation workflow, reasonable history-matching results were obtained for all 17 wells in Field A. The results indicated that the workflow could significantly

improve the simulation efficiency of a field-scale reservoir model with a complex natural fracture network throughout the entire production and injection process.
2. For a tight reservoir with complex natural fractures, the early production behavior of the horizontal wells might be impacted more by near-wellbore fractures, while the impact of matrix properties became more important for late-stage production.
3. Since the proposed simulation workflow is general, it has the potential to be applied to other unconventional reservoirs with complex fracture systems.

Acknowledgments

This work is supported by the North Dakota Industrial Commission's Oil and Gas Research Program and Eagle Energy Partners Tundra under the project, "Unitized Legacy Oil Fields: Prototypes for Revitalizing Conventional Oil Fields in North Dakota." The modeling work conducted under this program was made possible by contributions of software licenses from CMG, SimTech, and Schlumberger.

References

Begnaud, W. J. and Claiborne, E. B. 1985. September. Vertical Fracture Growth Considerations in the Mission Canyon/Ratcliffe Formations of the North Alexander Area. Presented at the SPE Annual Technical Conference and Exhibition, Las Vegas, Nevada, September. SPE-14375-MS. https://doi.org/10.2118/14375-MS.

Bera, A. and Belhaj, H. 2016. A Comprehensive Review on Characterization and Modeling of Thick Capillary Transition Zones in Carbonate Reservoirs. *J. Unconv. Oil and Gas Res*. **16**: 76–89.

Cho, Y., Apaydin, O. G. and Ozkan, E. 2013. Pressure-Dependent Natural-Fracture Permeability in Shale and its Effect on Shale-Gas Well Production. *SPE Res. Eval. & Eng*. **16** (02): 216–228. SPE-159801-PA.

Choi, E. S., Cheema, T. and Islam, M. R. 1997. A New Dual-Porosity/Dual-Permeability Model with Non-Darcian Flow Through Fractures. *J. Pet. Sci. and Eng*. **17** (3–4): 331–344.

Cinco-Ley, H., 1996. Well-Test Analysis for Naturally Fractured Reservoirs. *J. Pet. Technol*. **48** (01): 51–54.

Conlin, J. M., Hale, J. L., Sabathier, J. C., Faure, F. and Mas, D. 1990. October. Multiple-Fracture Horizontal Wells: Performance and Numerical Simulation. Presented at the European Petroleum Conference, The Hague, Netherlands, October. SPE-20960-MS. https://doi.org/10.2118/20960-MS.

Dakhelpour-Ghoveifel, J., Shegeftfard, M., and Dejam, M. 2019. Capillary-Based Method For Rock Typing In Transition Zone of Carbonate Reservoirs. *J. Pet. Exp. and Prod. Technol*. **9**: 2009–2018.

Fernández-Ibáñez, F., DeGraff, J. M. and Ibrayev, F. 2018. Integrating Borehole Image Logs with Core: A Method to Enhance Subsurface Fracture Characterization. *AAPG Bulletin* **102** (6): 1067–1090.

Gale, J., Elliott, S., Li, J. Z., and Laubach, S. 2019. July. Natural fracture characterization in the wolfcamp formation at the hydraulic fracture test site (HFTS). Presented at the SPE/AAPG/SEG Unconventional Resources Technology Conference, Denver, Colorado, USA, July. URTEC-2019-644-MS. https://doi.org/10.15530/urtec-2019-644.

Hendricks, M. L. 1988. Shallowing-Upward Cyclic Carbonate Reservoirs in the Lower Ratcliffe Interval (Mississippian), Williams and McKenzie Counties, North Dakota. Occurrence and Petrophysical Properties of Carbonate Reservoirs in the Rocky Mountain Region.

Fernandez-Ibanez, F. and DeGraff, J. M. 2016. November. Using a Genetic-Based Approach to Enhance Natural Fracture Characterization in a Giant Carbonate Field. Presented at the SPE Annual Caspian

Technical Conference & Exhibition, Astana, Kazakhstan, November. SPE-182565-MS. https://doi.org/10.2118/182565-MS.

Hirsch, J. M., Cisar, M. T., Glass, S. W., and Romanowski, D. A. 1981. October. Recent Experience with Wireline Fracture Detection Logs. Presented at the SPE Annual Technical Conference and Exhibition, San Antonio, Texas, October. SPE-10333-MS. https://doi.org/10.2118/10333-MS.

Ibrayev, F., Fernandez-Ibanez, F. and DeGraff, J.M., 2016, November. Using a genetic-based approach to enhance natural fracture characterization in a giant carbonate field. presented at the SPE Annual Caspian Technical Conference & Exhibition, Astana, Kazakhstan. SPE-182565-MS. https://doi.org/10.2118/182565-MS.

Jarvie, D. M., Lefever, J., and Nordeng, S. H. 2016. Madison Group Source Rocks, Williston Basin, USA. Presented at the AAPG Annual Convention and Exhibition, Calgary, Alberta, Canada, June.

Jia B., Jin L., Mibeck, B. A., Smith, S. A., and Sorensen, J. A. An Integrated Approach of Measuring Permeability of Naturally Fractured Shale. 2020. *J. Pet. Sci. and Eng*. **186**: 106716.

Jia, B., Jin, L., Smith, S. A., and Bosshart, N. W. 2021. Extension of the Gas Research Institute (GRI) Method to Measure the Permeability of Tight Rocks. *J. Natur. Gas. Sci. and Eng*. **91**: 103756.

Jin, L. and Wojtanowicz, A. K., 2014. Progression of Injectivity Damage with Oily Waste Water in Linear Flow. *Pet. Sci*. **11**: 550–562.

Jin, L., Jiang, T., Dotzenrod, N., Patil, S., Klenner, R., Sorensen, J., and Bosshart, N. 2019. Modeling Study of the Unconventional Bakken Formation for Gas Injection EOR. *Pet. Geostat. 2019* (1): 1–5.

Jin, L., Kurz, B. A., Ardali, M., Wan, X., Zhao, J., He, J., Hawthorne, S. B., Djezzar, A. B., Yu, Y., and Morris, D. 2022a. Investigation of Produced Gas Injection in the Bakken for Enhanced Oil Recovery Considering Well Interference. Presented at the SPE/AAPG/SEG Unconventional Resources Technology Conference, Houston, Texas, USA, June. URTEC-3723697-MS. https://doi.org/10.15530/urtec-2022-3723697.

Jin, L., Wan, X., Azzolina, N. A., Bosshart, N. W., Zhao, J., Yu, Y., Yu, X., Smith, S. A., Sorensen, J. A., and Gorecki, C. D. 2022b. Optimizing Conformance Control for Gas Injection EOR in Unconventional Reservoirs. *Fuel* **324**: 124523.

Lie, K. A. and Møyner, O. eds., 2021. Advanced Modelling with the MATLAB Reservoir Simulation Toolbox. Cambridge University Press.

Liu, C. 2020. Automatic History Matching with Data Integration for Unconventional Reservoirs. Master Thesis. The University of Texas at Austin, Austin, Texas.

Liu, C., Gupta, A., Ates, H., Yu, W., Li, N., and Sepehrnoori, K. 2022. February. Automatic Calibration of Complex 3D Discrete Fracture Networks using EDFM-AI. Presented at the International Petroleum Technology Conference, Riyadh, Saudi Arabia, February. IPTC-22183-MS. https://doi.org/10.2523/IPTC-22183-MS.

Lynn, H. B., Bates, R., Layman, M., and Jones, M. 1995. Natural Fracture Characterization Using P-Wave Reflection Seismic Data, VSP, Borehole Imaging Logs, and the In-Situ Stress Field Determination. Presented at the Low Permeability Reservoirs Symposium, Denver, Colorado, March. SPE-29595-MS. https://doi.org/10.2118/29595-MS.

Ma, S., Ju, B., Zhao, L., Lie, K. A., Dong, Y., Zhang, Q., and Tian, Y., 2022. Embedded Discrete Fracture Modeling: Flow Diagnostics, Non-Darcy Flow, and Well Placement Optimization. *J. Pet. Sci. and Eng*. **208**, p. 109477.

Masalmeh, S. K., Shiekah, I. A., and Jing, X. D. 2007. Improved Characterization and Modeling of Capillary Transition Zones in Carbonate Reservoirs. *SPE Res. Eval. & Eng*. **10** (02): 191–204.

Mohamed, A. A. I., Belhaj, H., Gomes, J. S., and Bera, A. 2017. Petrographic and Diagenetic Studies of Thick Transition Zone of a Middle-East Carbonate Reservoir. J. *Pet. and Gas Eng*. **8** (1): 1–10.

Mirzaei, M. and Cipolla, C. L. 2012. January. A Workflow for Modeling and Simulation of Hydraulic Fractures in Unconventional Gas Reservoirs. Presented at the SPE Middle East Unconventional Gas Conference and Exhibition, Abu Dhabi, UAE, January. SPE-153022-MS. https://doi.org/10.2118/153022-MS.

Narr, W., Schechter, D. S., and Thompson, L. B. 2006. Naturally Fractured Reservoir Characterization. *Soc. Pet. Eng*. https://doi.org/10.2118/9781613999615.

Nie, R. S., Meng, Y. F., Jia, Y. L., Zhang, F. X., Yang, X. T., and Niu, X. N., 2012. Dual Porosity and Dual Permeability Modeling of Horizontal Well in Naturally Fractured Reservoir. *Transport in Porous Media* **92**: 213–235.

Oliver, D. S. and Chen, Y. 2011. Recent Progress on Reservoir History Matching: A Review. *Computational Geosciences* **15**: 185–221.

Ray, D. S., Al-Shammeli, A., Verma, N. K., Matar, S., De Groen, V., De Joussineau, G., Ghilardini, L., Le Maux, T., and Al-Khamees, W. 2012. Characterizing and Modeling Natural Fracture Networks in a Tight Carbonate Reservoir in the Middle East: A Methodology. *Bulletin of the Geological Society of Malaysia* **58** (58): 29–35.

Shi, S., Belhaj, H., and Bera, A. 2018. Capillary Pressure and Relative Permeability Correlations for Transition Zones of Carbonate Reservoirs. *J. Pet. Explor. and Prod. Technol*. **8**: 767–784.

Spearing, M. C., Abdou, M., Azagbaesuweli, G., and Kalam, M.Z. 2014. November. Transition Zone Behaviour: The Measurement of Bounding and Scanning Relative Permeability and Capillary Pressure Curves at Reservoir Conditions for a Giant Carbonate Reservoir. Presented at the Abu Dhabi International Petroleum Exhibition and Conference, Abu Dhabi, UAE, November. SPE-171892-MS. https://doi.org/10.2118/171892-MS.

Sun, J., Schechter, D., and Huang, C. K. 2016. Grid-Sensitivity Analysis and Comparison Between Unstructured Perpendicular Bisector and Structured Tartan/Local-Grid-Refinement Grids for Hydraulically Fractured Horizontal Wells in Eagle Ford Formation with Complicated Natural Fractures. *SPE J*. **21** (06): 2260–2275.

Tao, Q., Ghassemi, A., and Ehlig-Economides, C. A. 2011. A Fully Coupled Method to Model Fracture Permeability Change in Naturally Fractured Reservoirs. *International J. Rock Mechan. and Mining Sci*. **48** (2): 259–268.

Tripoppoom, S., Yu, W., Sepehrnoori, K., and Miao, J. 2019. July. Application of Assisted History Matching Workflow to Shale Gas Well Using EDFM and Neural Network-Markov Chain Monte Carlo Algorithm. Presented at the SPE/AAPG/SEG Unconventional Resources Technology Conference, Denver, Colorado, USA, July. URTEC-2019-659-MS. https://doi.org/10.15530/urtec-2019-659.

Vavra, C. L., Kaldi, J. G., and Sneider, R. M. 1992. Geological Applications of Capillary Pressure: A Review. *AAPG Bulletin* **76** (6): 840–850.

Wan, X. 2020. Coupled Simulation of Hydraulic Fracturing, Production, and Refracturing for Unconventional Reservoirs. Doctoral Dissertation. The University of North Dakota.

Wan, X., Jin, L., Azzolina, N. A., Butler, S. K., Yu, X., and Zhao, J. 2022. Applying Reservoir Simulation and Artificial Intelligence Algorithms to Optimize Fracture Characterization and CO_2 Enhanced Oil Recovery in Unconventional Reservoirs: A Case Study in the Wolfcamp Formation. *Energies* **15** (21): 8266.

Wan, X., Rasouli, V., Damjanac, B., Yu, W., Xie, H., Li, N., Rabiei, M., Miao, J., and Liu, M. 2020. Coupling of Fracture Model with Reservoir Simulation to Simulate Shale Gas Production with Complex Fractures and Nanopores. *J. Pet. Sci. and Eng*. **193**: 107422.

Warren, J. E. and Root, P. J. 1963. The Behavior of Naturally Fractured Reservoirs. *Soc. of Pet. Eng. J*. **3** (03): 245–255.

Woo, G. T. and Cramer, D. D. 1984. May. Laboratory and Field Evaluation of Fluid-Loss Additive Systems Used in the Williston Basin. Presented at the SPE Rocky Mountain Regional Meeting, Casper, Wyoming, May. SPE-12899-MS. https://doi.org/10.2118/12899-MS.

Xu, Y., 2015. Implementation and Application of the Embedded Discrete Fracture Model (EDFM) for Reservoir Simulation in Fractured Reservoirs. Master Thesis, the University of Texas – Austin.

Xu, Y., Cavalcante Filho, J. S., Yu, W., and Sepehrnoori, K. 2017. Discrete-Fracture Modeling of Complex Hydraulic-Fracture Geometries in Reservoir Simulators. *SPE Res. Eval. & Eng*. **20** (02): 403–422.

Yu, W., Luo, Z., Javadpour, F., Varavei, A., and Sepehrnoori, K. 2014. Sensitivity Analysis of Hydraulic Fracture Geometry in Shale Gas Reservoirs. *J. Pet. Sci. and Eng*. **113**: 1–7.

Zhang, S., Pu, H., and Zhao, J. X. 2019. Experimental and Numerical Studies of Spontaneous Imbibition with Different Boundary Conditions: Case Studies of Middle Bakken and Berea Cores. *Energy & Fuels* **33** (6): 5135–5146.

Zhang, S., Li, Y., and Pu, H. 2020. Studies of the Storage and Transport of Water and Oil in Organic-Rich Shale Using Vacuum Imbibition Method. *Fuel* **266**: 117096.

Zhao, B., Shang, Y., Jin, L., and Jia, B. 2017. Characterizing Connectivity of Multiscale Pore Structure in Unconventional Reservoirs by the Complex Network Theory. Presented at the SPE/AAPG/SEG Unconventional Resources Technology Conference, Austin, Texas, USA, July. URTEC-2665304-MS. https://doi.org/10.15530/URTEC-2017-2665304.

Zhao, J., Jin, L., Azzolina, N. A., Wan, X., Yu, X., Sorensen, J. A., Kurz, B. A., Bosshart, N. W., Smith, S. A., Wu, C., Vrtis, J. L., Gorecki, C. D., and Ling, K. 2022. Investigating Enhanced Oil Recovery in Unconventional Reservoirs Based on Field Cases Review, Laboratory and Simulation Studies. *Energy & Fuels* **36** (24): 14771–14788.